Microstructure and properties of styrene acrylate polymer cement concrete

Zhao Su
Faculty of Civil Engineering, Delft University of Technology, The Netherlands

The paper systematically describes the evolution of the microstructure of a styrene acrylate polymer cement concrete in relation to its mechanical properties and durability. The results presented and discussed at the present paper involve the interaction of the polymer dispersion with portland cement; the effect of the polymer modification on the hydration of cement; the evolution of the microstructure of polymer cement pastes at the early stage; the interface, pore structure, mechanical properties and freeze-thaw (F-T) resistance of polymer cement concrete (PCC). The objective of this investigation is to arrive at a better understanding of the microstructure of PCC and the way in which the microstructure develops. Furthermore, an attempt has been made to relate the micro-structure of concrete to its mechanical properties and durability aspects, such as F-T resistance.

Keywords: **microstructure, polymer dispersion, cement concrete, mechanical properties, freeze/thaw**

1 Introduction

The use of polymer dispersions in concretes and mortars dates back to the 1920s (Lefebure, 1924). In those days, natural rubber dispersions were used. Extensive research and development of polymer cement concrete (PCC) have been carried out since the invention of synthetic polymer dispersions in the late 1940s, especially in the last three decades. In practice, the level of polymer dosages, based on the mass ratio of polymer solids to cement, ranges from 5-20%, of which 10–20% appears to be found to yield optimum performance. PCC is widely applied for overlays on road structures, floors, repairs, glass fibre reinforced composites etc. The polymer improves a number of properties of concrete, such as adhesion strength to various substrates, impermeability, strain capacity, impact strength, abrasion resistance, and meanwhile decreases water absorption and chloride penetration. Consequently, PCC generally exhibits excellent mechanical properties and durability, such as freeze-thaw (F-T) deicing salt resistance.

Several models (Ohama 1987, Dingley 1974, Grookurth 1989 & Lavelle 1988) and a number of strengthening mechanisms have been proposed to describe the evolution of microstructure and mechanical properties of the PCC. The possible mechanisms can be summarized as follows:

- The formation of a polymer film at the interface improves the bond strength between cement paste and aggregates (Ohama 1987, Su et al 1990, 1991, 1994, Isengerg et al 1973 & Bijen 1991);

- A continuous polymer phase is formed within the cement matrix. The microcracks in PCC's under stress are bridged by the formed polymer film, which inhibits the crack propagation (Ohama 1987, Bentur 1990 & Isengerg et al 1973);
- The addition of polymer improves the workability of the mix and less water is required, leading to strength improvements (Isengerg et al 1973, Nany et al 1978, Popovics et al 1978 & Bijen 1991);
- Another effect could be that the structure of concrete becomes more homogeneous so that local stress concentrations are decreased. Also, stress dissipation at crack tips in the soft polymer crossing the brittle cement hydrates can be a cause for more homogenous stress distribution (Bijen 1994).

However, the exact strengthening mechanism of polymers in PCC has not been firmly identified (Mai et al 1986). The process and mechanism by which the microstructure develops, and how it is related to the properties is still a topic of ongoing research. The objective of this investigation is to arrive at a better understanding of the microstructure of PCC and the way in which the microstructure develops. Furthermore, an attempt has been made to relate the microstructure of concrete to its mechanical properties and durability. The latter concerns freeze-thaw (F-T) resistance with and without deicing salt.

2 Materials

Materials used in this investigation included: portland cement Type CEM I 32.5, equivalent to portland cement ASTM Type I, and a styrene acrylate (SA) dispersion supplied by Forton BV in Holland. The SA polymer dispersion has a solid content of 48.6% by mass of the dispersion (at 105 °C drying), a pH value of 8.5 and an average particle size of 0.27 μm. The polymer consists of 50% styrene and 50% butyl acrylate. The dispersion is a non-ionic type, containing a defoaming agent. A superplasticizer, NV-BETOMIX 415 (a sulphonated naphthalene formaldehyde condensate) supplied by VN-PCI BV in Holland, was used to reduce the water demand in the reference concrete. Rhine river sand and gravel were used as aggregates.

3 Experiments

3.1 *Mix design and cure of specimens*

The mix compositions of cement paste and concrete mixtures are given in Tables 1 and 2, respectively. The polymer content is expressed as the percentage of the mass ratio of polymer solids to cement (p/c). The water contained in the polymer dispersion has been considered for the calculation of water cement ratios (w/c). The gradation of aggregates (D_{max} = 16 mm) is in accordance with the Dutch standard NEN 5950 (Su 1995). Prism concrete specimens (100 × 100 × 300 mm) were prepared according to the ASTM Standard C 192-81 for the F-T tests.

The specimens were cured for 1 day at the ambient temperature, with the top surface covered by a piece of plastic sheet to prevent water from evaporating. After demoulding at 1 day, subsequent curing was done in a climate room (at 20°C 65% relative humidity) till testing.

Table 1. The mix proportions of cement pastes.

	cement	total water	polymer content (%)		
mix no.	volume percent		p/c	v/v^*	w/c
1	50.6	47.9	0	0	0.30
2	46.7	43.9	5.7	8.0	0.30
3	42.9	40.7	11.2	14.9	0.30
4	37.9	35.8	22.0	24.8	0.30
5	46.1	36.4	11.2	16.0	0.25
6	40.3	31.8	22.0	26.4	0.25

Note: v/v means the volume ratio of polymer solids to the whole of the polymer cement paste. For the sake of comparison with previous results, v/v is listed next to the column of the p/c.

Table 2. The mix compositions and properties of fresh concretes.

mix no.	A	B	C	D	E	F
w/c	0.44	0.44	0.44	0.44	0.33	0.28
p/c (%)	0	5.7	11.2	22.0	11.2	22.0
mix compositions (kg/m^3)						
cement	331	329	325	314	332	323
SA dispersion	0	38.9	78.1	142.4	79.6	146.1
polymer solids	0	18.9	37.9	69.2	38.7	71.0
total water	145.6	145.2	143.3	138.7	109.5	90.5
aggregates	1925	1890	1866	1805	1903	1852
anitifoamer	1.6	1.8	1.8	1.8	1.9	1.9
superplasticizer	4.9	0	0	0	0	0
total	2383	2385	2374	2329	2385	2338
air content (%)	2.68	1.83	1.31	1.52	2.98	4.11
slump (mm)	35	180	235	260	30	45

3.2 *Experimental techniques*

The adsorption of polymer particles to the surface of cement grains was investigated with the Coulter LS 130 particle analyzer and a filtration technique (Su 1995 & Su et al 1992). The cement hydration was studied by determining the non-evaporable water content (Su et al 1991a) and free-CaO

content of the paste (Franke 1941). The evolution of microstructure of polymer cement paste was characterised with an environmental scanning electron microscope (ESEM) and a scanning electron microscope (SEM) (Su 1995, Su et al 1993 & 1995), while the interface between the paste and aggregates (limestone and granite) was examined with the SEM (Su 1995). The pore structure of the paste and concrete was determined by the Mercury Porosimeter (Pore Sizer 9320) (Su 1995 & Su et al 1994). A tension machine Instron 1122, with a 5 kN capacity and a special mounting device, was used to measure the adhesion strength (Su 1995 & Su et al 1991b).

The F-T test was carried out in conformity with the RILEM Recommendation: "Methods of carrying out and reporting F-T tests on concrete with and without de-icing chemicals solution" (Lavitt, 1974). The F-T cycle consists of a freezing time of 16 hours at a minimum temperature of –16 °C and a thawing time of 8 hours at a maximum temperature of 5 °C (24 hours a cycle). Before and after 10, 20, 25, 30, 40, 50 F-T cycles without deicing salt, the water absorption and the transition time of an ultrasonic pulse of concrete specimens were measured. The water absorption was calculated by simply adding up the increase in weight divided by the surface area. The transition time was determined with an apparatus C.S.I. Concrete Tester, Type RBT-3 over 30 cm length (Fraaij 1990). For the F-T test with deicing salt (3% of NaCl solution), the surface weight loss was measured.

The modulus of rupture (bending strength) and compressive strength were determined in accordance with the ASTM standard C 193-79 before the F-T test and after 50 cycles of the F-T test without deicing salt. The effects of D-W treatment (dried in an oven at 90 °C for 7 days and then immersed in water at 20 °C for another 7 days) on the compressive strength, the loss and adsorption of free water of plain concrete and PCC's were also studied.

4 Results

4.1 *Adsorption of polymer particles to the surface of cement grains*

Fig. 1 presents the results of the Coulter analysis on 11.2% of polymer SA cement paste ($w/c = 0.30$) both soon and 2 hours after mixing, compared with the raw cement and calculated results. In this mixture, the solid polymer accounts for 25.7% of total solid volume (polymer+ cement). The calculated curve is based on 25.7% of the polymer and 74.3% of cement at the various particle size. In the polymer SA modified paste, both soon and 2 hours after mixing, there is a distinct peak of particle distribution in the range of 0.1–0.8 μm. Obviously this concerns free or non-adsorbed polymer particles. The main peaks in the range of about 10–100 μm are associated with cement. The graph shows that a part of polymer particles is adsorbed on the surface of cement grains directly after mixing in comparison of experiment curves (No. 1 and 2) with the calculated one (No. 3).

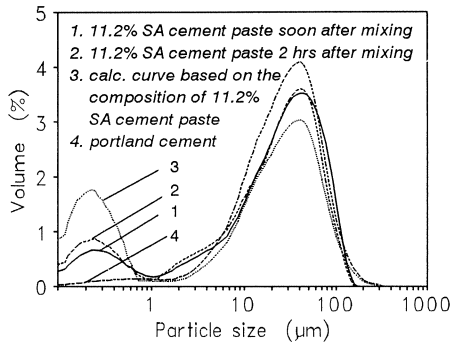

Fig. 1. The particle size distribution of portland cement and polymer cement paste.

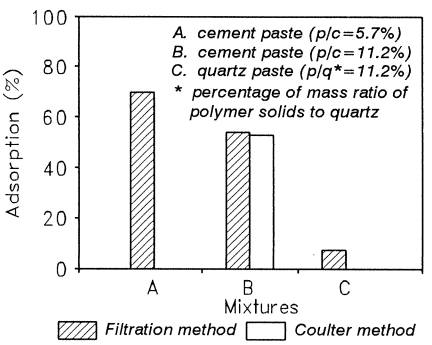

Fig. 2. The percentage of polymer adsorbed onto the surface of cement and quartz particles.

Fig. 2 represents the amount of the polymer adsorbed onto cement by means of the filtration and Coulter techniques. The percentage of polymer adsorbed onto the surface of cement grains as measured with the Coulter LS 130 have been further confirmed by the filtration test on the supernatant of cement suspensions as shown in Fig. 2. The results of both methods are quite similar for the paste with 11.2% of polymer. Also, it can be seen that the amount of polymer adsorbed on quartz particles is much lower than that on cement grains.

4.2 *Effect of polymer addition on the hydration of cement*

Fig. 3 summarizes the results of the degree of cement hydration as a function of age in days. With increasing SA contents the hydration rate of cement decreases, especially at the early stage of hydration. After 28 days the cement hydration process proceeds slowly. This applies to both the modified and the unmodified pastes. For instance, from 28 to 90 days, the degrees of hydration of unmodified paste and of the paste modified with 22.0% of SA polymer are 66.4–66.7% and 48.8–49.9%, respectively.

Fig. 4 shows the free-lime content present in the hydrated pastes as a function of the hydration time in days. After 7 days of hydration, the amount of free-lime becomes nearly constant. The addition of 10% silica fume to cement significantly reduces the amount of free-lime, owing to the secondary reaction of silica fume with calcium hydroxide released by the hydration of cement. The free-CaO content decreases with an increase in SA content at 1 day. But it is obvious from the figure that the amount of free-lime in the paste modified with 5.7% and 11.2% of SA exceeds that in the unmodified paste after 7 and 28 days of hydration, respectively. This result is in conflict with the degree of hydration results which were estimated on the basis of the non-evaporable water content in the pastes.

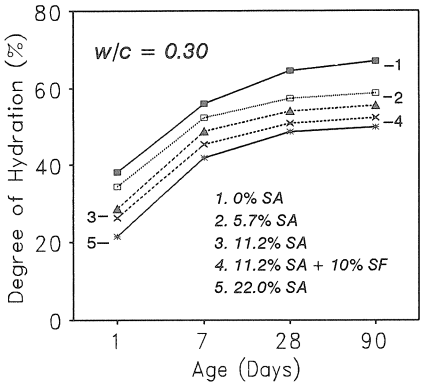

Fig. 3. Degree of cement hydration as a function of age (days).

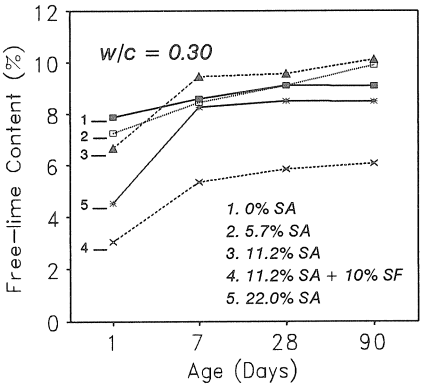

Fig. 4. Free lime constant of SA *cement pastes as a function of age (days).*

4.3 Evolution of the microstructure of polymer cement pastes at the early stage

4.3.1 Four hours after mixing

Fig. 5 (A) shows that, after 4 hours of hydration, tiny C-S-H gel can be seen on the surface of cement grains of the control paste. While the paste modified with 11.2% of polymer, as shown in Fig. 5 (B) demonstrates that cement grains are covered by a thin layer of diffuse amorphous polymer phase with some hydration products. The polymer film is formed due to the hydration of cement and the partial drying as capillary pore water evaporates in the chamber of microscope.

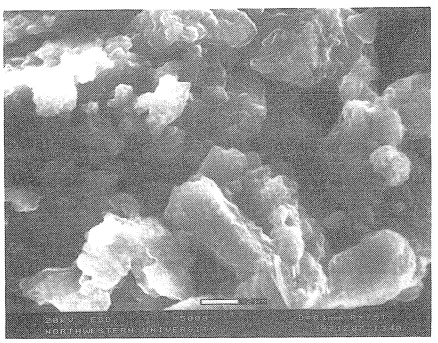

(A) p/c = 0%

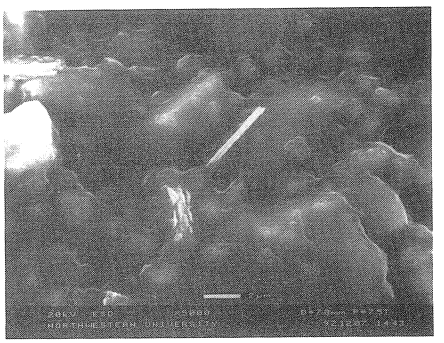

(B) p/c = 11.2%

Fig. 5. The ESEM *micrographs showing the structure of cement pastes at 4 hours after mixing.*

Fig. 6 presents SEM micrographs showing the structure of cement pastes without and with 11.2% of polymer at 4 hours after mixing. Fig. 6 (A) shows, on one hand, tiny and fur-like hydration products which are formed on the surface of cement grains, on the other hand, remarkable micro-cracks grow through the space among cement grains due to the pretreatment of the specimen, indicating serious structure damage. While Fig. 6 (B) exhibits that cement grains are almost covered with a thin layer of polymer film. Furthermore, the figure also shows that the polymer film bridges up three pieces of cement grains.

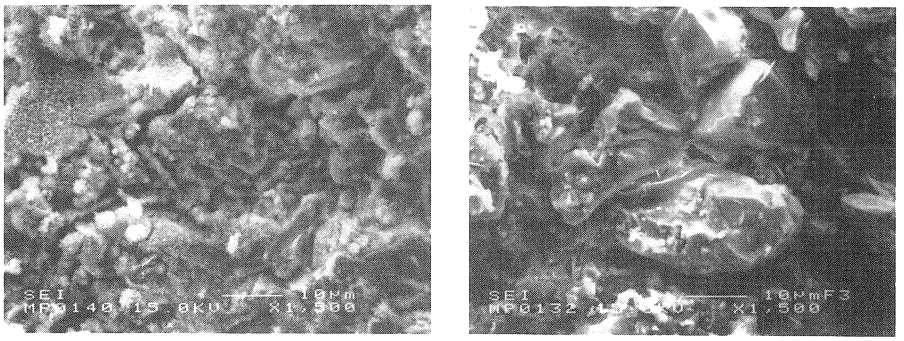

(A) p/c = 0% *(B) p/c = 11.2%*

Fig. 6. The SEM micrographs showing the structure of cement pastes 4 hours after mixing.

4.3.2 One day after mixing

After one day, C-S-H gel in the control paste is well developed on the surface of cement grains and in the "neck regions" between cement grains, and well developed crystals of calcium hydroxide have precipitated as shown in Fig 7 (A). In the polymer modified pastes as shown in Fig. 7 (B) and (C), reaction products are now abundant. Fig 7 (B) shows that, in the paste with 5.7% polymer, the structure is essentially similar to that of the control. Polymer is not distinguishable, indicating that it is almost completely engulfed by or incorporated into C-S-H gel and other products. The addition of polymer seems to encourage the growth of straight, parallel, sheets- and fibre-like structures as shown in Fig. 7 (C). In the paste with 22.0% of polymer, however, no hydration products are observed and cement particles appear to be covered by the polymer as seen in Fig. 7 (D). Also, the polymer film fills the interstices between cement grains and bridges capillary pores.

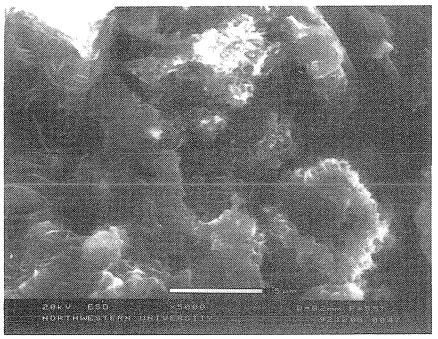

(A) $p/c = 0\%$

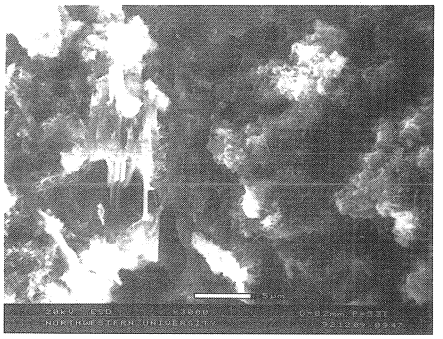

(B) $p/c = 5.7\%$

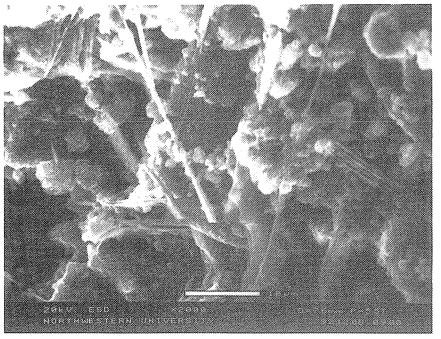

(C) $p/c = 11.2\%$

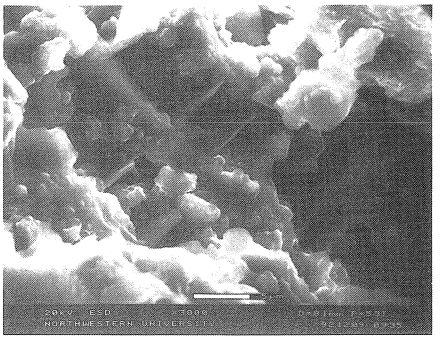

(D) $p/c = 22.0\%$

Fig. 7 The ESEM micrographs showing the structure of cement pastes at 1 day after mixing.

4.4 *Microstructure at the interface of PCC in the hardened stage*

Fig. 8 shows the microstructure of the fractured interface between plain cement paste and aggregates. Graphs (A) and (B) refer to the composite with limestone and granite, respectively. In the case of granite, a porous interfacial layer appears to be present as compared with limestone.

Fig. 9 shows the microstructure of the interface between polymer cement paste ($p/c = 22.0\%$) and aggregates. Fig. 9 (B) exhibits the granite-paste interface, where a continuous polymer film appears to be present, which seems to screen off the hydrates, such as ettringite. Fig. 9 (A) shows the limestone-paste interface, indicating location "A" is denser than "B". On the latter location a thin layer of the paste appears to be detached away with the aggregate. The cement hydration products are almost entirely covered by the polymer. In comparison, the interface of PCC is much denser than that of plain concrete, especially in the case of granite as shown in Fig. 8.

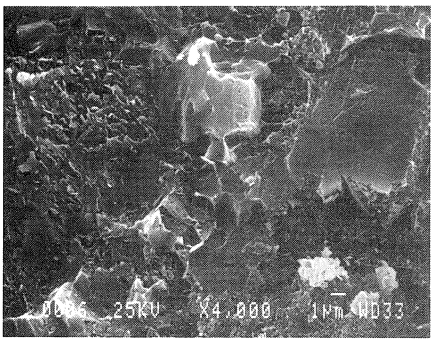

(A) Limestone

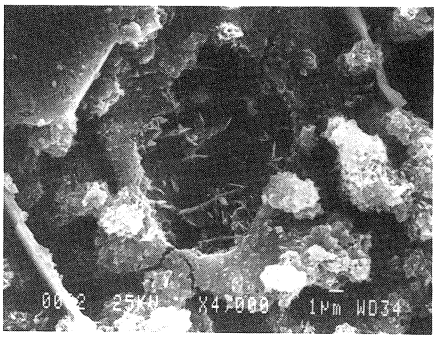

(B) Granite

Fig. 8. SEM *micrographs of fractured interfaces between plain cement paste and aggregates for 28 days old composites.*

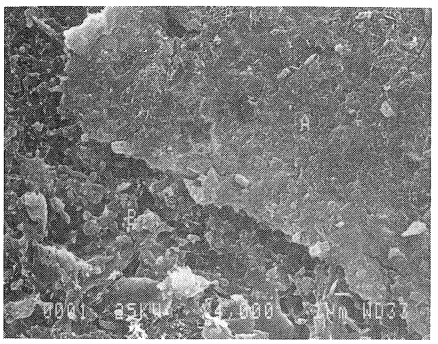

(A) Limestone

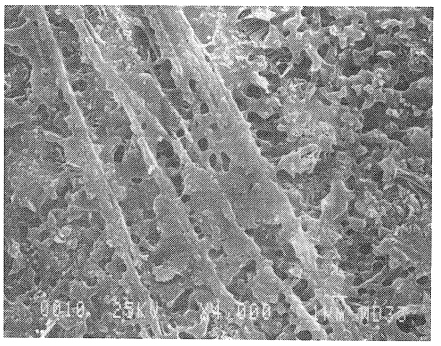

(B) Granite

Fig. 9. SEM *micrographs of fractured interfaces between polymer cement paste (p/c = 22%) and aggregates for 28 days old composites.*

Fig. 10 presents a SEM micrograph showing the structure of the interface of PCC on the polymer cement paste ($p/c = 11.2\%$) side. This specimen (at 28 days) was treated with 0.1 N HCl solution for 1 hour to remove the cementitious components before observing with the SEM (Su et al 1992a). As can be seen from the figure the polymer film appears to bridge and block a capillary pore, where the hydration products, developed during the hydration of cement, have been etched away.

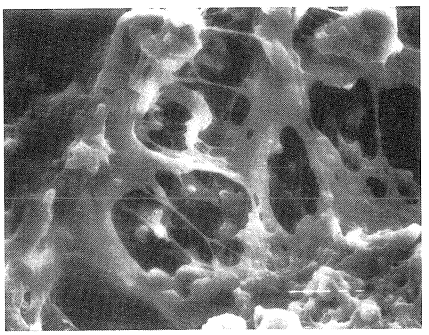

Fig. 10. SEM micrograph showing the structure of polymer film formed in hardened cement paste.

4.5 *Adhesion strength of polymer cement pastes to aggregates*

Fig. 11 shows the influence of polymer SA contents on the development of adhesion strength of cement paste to limestone (A) and granite (B) up to 180 days. It is evident that the adhesion strength depends on the polymer content, type of aggregates, and age of the composites. The adhesion strength of the modified paste with 22.0% of polymer SA, both in the case of limestone and granite, is significantly improved. For instance, the adhesion strength of cement paste with 22.0% of polymer SA to granite is even greater than the tensile strength of granite (3.8 N/mm^2) used as aggregate in the investigation (Su et al 1991b). It also can be seen that, in the case of granite, the adhesion strength increases with increasing polymer loading after 7 days. However, the increase in the adhesion strength slows down after 90 days. While in the case of limestone, the adhesion strength is significantly improved only for the paste with 22.0% of the polymer. On the contrary, the adhesion strength of plain cement paste to both kinds of rocks under the same curing condition falls to zero at the age of 28 days.

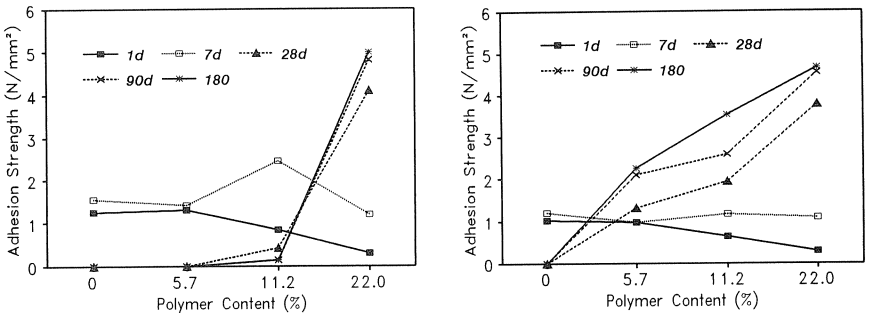

(A) to limestone *(B) to granite*

Fig. 11. Effect of polymer SA addition on the adhesion strength of cement pastes to aggregates.

4.6 *Pore structure of polymer cement paste and concrete*

Figs. 12 and 13 show effects of polymer contents and water/cement ratios on the pore size distribution of cement paste and concrete at 28 days, respectively. The cumulative intruded volumes are plotted against the pore diameter (μm) in logarithmic scale.

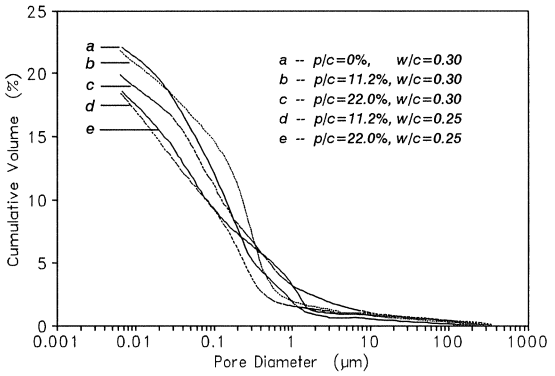

Fig. 12. Effects of polymer contents and w/c ratios on the pore size distribution of cement pastes.

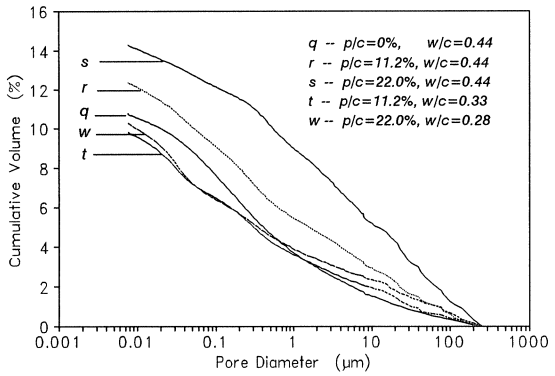

Fig. 13. Effects of polymer contents and w/c ratios on the pore size distribution of cement concrete. The samples (with sizes around 5–10 mm) were carefully selected from base concrete specimens (coarse aggregates are picked out as far as possible)

4.6.1 Effects of polymer content and water/cement ratio on the pore structure of cement paste

Fig. 12 shows that, for cement pastes with a constant water/cement ratio (0.30), the total intruded volume decreases with increasing polymer content. However, the volume of pores with a size

larger than 1 μm slightly increases, while the volume of pores intruded with a size smaller than 0.03 μm decreases with increasing polymer loading, particularly for the paste with 22.0% of polymer. It is apparent that the pores around 100 μm are associated with air entrainment.

At increasing polymer content the total intruded volume of the paste decreases. This corresponds with the decrease in the amount of cement and water in the pastes when the polymer content increases, as shown in Table 1. The results indicate that polymer cement pastes appear to give more easy access to mercury intrusion than the pure cement paste.

If the polymer cement pastes are prepared at the same level of workability as that of plain cement paste, in which case the water/cement ratio decreases at increasing polymer content, a substantial decrease in the intruded porosity is observed. Polymer cement paste, with p/c = 11.2% and w/c = 0.25, has the same workability (flow size) as that of plain cement paste, the total intruded porosity of the former is about 4% lower than that of the later. For the pastes both with 11.2% of polymer, but different water/cement ratios, e.g. 0.30 and 0.25, respectively, the difference in intruded porosity is about 3.5%. Therefore, the reduction of the water/cement ratio is the main cause for the decrease in the intruded porosity.

4.6.2 Effects of polymer content and water/cement ratio on the pore structure of cement concrete

Fig. 13 demonstrates that, at a constant water/cement ratio, the total intruded volume of PCC's nearly proportionally increases with increasing polymer contents from 0% to 22.0%. For instance, the total porosity of plain concrete is 10.7%, while it is 14.3% for PCC with 22.0% of polymer at the same w/c. Furthermore, the volume of pores with sizes larger than 1 μm significantly increases, e.g. for PCC with 22.0% of polymer (w/c = 0.44), the volume of pores larger than 1 μm is 9.0%, whereas for plain concrete, it is only 3.7%. As can be seen from the figure the pattern of the pore size distribution of PCC's is different from that of polymer cement pastes (see Fig. 12). In contradiction to the pastes, PCC's and unmodified concrete do not show the distinctive threshold diameter, beyond which the intruded pore volume increases steeply. For example for the PCC with p/c = 22.0% and w/c = 0.44, the cumulative volume increases almost linearly against pore diameters from 0.2 μm to 200 μm. Afterwards, the increase appears to slow down.

If the workability of PCC's is maintained at the same level as that of plain concrete (with a slump value of 30–45 mm), by adjusting the water/cement ratio, the total porosity of PCC will decrease. For the PCC with p/c = 11.2% and w/c = 0.33, the total intruded volume and the volume of pores larger than 1 μm is 9.8% and 3.6%, respectively, whereas for plain concrete, it is 10.7% and 3.7%, respectively. A further increase of polymer dosage from 11.2% (w/c = 0.33) to 22.0% (w/c = 0.28) does not show a further positive effect on the pore structure of PCC's. On the contrary, the total intruded volume increases.

4.7 *F-T Resistance of PCC's*

4.7.1 Moisture variation in PCC's

The characteristics of water absorption and loss of free water of specimens are of importance with regard to the F-T resistance. Fig. 14 presents the loss of free water of concrete specimens at 28 days as a function of drying time. The specimens are dried in an oven at 90 °C for 7 days. As can be seen from the figure the amount of lost water decreases significantly with increasing polymer contents. The reference concrete (No. A) shows the highest loss. The loss of free water also decreases with reducing water/cement ratios.

Fig. 15 shows the water absorption of the concrete specimens (after drying in an oven at 90 °C for 7 days) as a function of time immersed in water at 20 °C. The results show that the absorption of the reference concrete (No.A) is much higher than that of PCC's. For example at 1 day, the absorption of plain concrete nearly reaches a value of 170 mg/cm^2, thereafter water absorption is very limited. However, for the PCC with a polymer content of 5.7%, the amount of absorbed water is only about half of plain concrete at 1 day. After 1 day, PCC's continue to absorb water, but very slowly. Furthermore, it is evident that the amount of absorbed water significantly decreases with increasing polymer content and decreasing water/cement ratio.

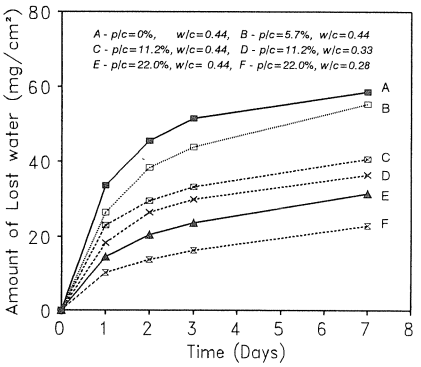

Fig. 14. The amount of free water lost in specimens during drying in an oven at 90°C as a function of time (days).

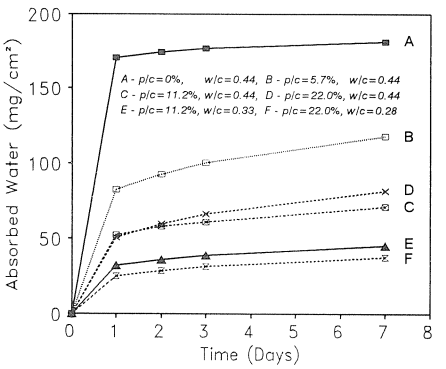

Fig. 15. The amount of water absorbed in specimens (after drying at 90°C) immersed in water at 20°C as a function of time (days).

Fig. 16 presents the results of the water absorption of concretes as a function of the number of F-T cycles without deicing salt. Before the commencement of the F-T cycling, the specimens were immersed in water for 2 days. As can be seen in the figure during the immersion period of 2 days the water absorption is fast, thereafter slows down during the F-T cycling. The water absorption significantly decreases with increasing polymer content and with decreasing water/cement ratio.

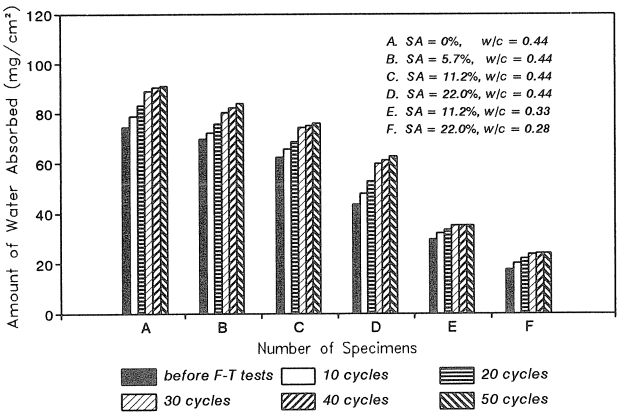

Fig. 16. The amount of water absorbed in concrete specimens after a period of 2 days of immersion in water and during the F-T cycling.

The results presented in Figs. 14–16 show that polymer modification significantly retards the process of water evaporation and absorption of concretes. This undoubtedly is beneficial for the F-T resistance of concretes. The effect of this phenomenon is that when concrete freezes, the water content of PCC will be lower than that of the unmodified. Consequently, the resistance to freezing will be higher.

4.7.2 F-T resistance of PCC's in the presence of deicing salt

Figs. 17 to 19 present the results of the surface weight loss of concrete specimens as a function of the number of F-T cycles with deicing salt. They refer to the results of the top, side and bottom surface of concretes, respectively. According to the RILEM recommendation, concretes with good scaling resistance must have a surface weight loss lower than 0.2 mg/mm^2 after F-T tests [Lavitt, 1974].

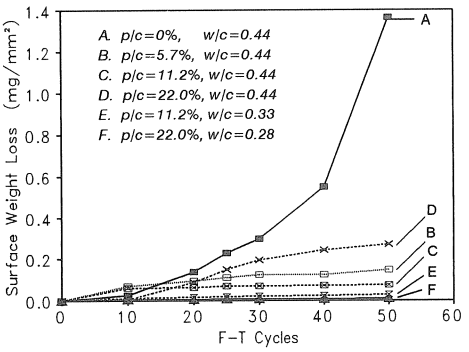

Fig. 17. The top surface weight loss of concrete specimens as a function of the number of F-T cycles with deicing salt.

Fig. 17 shows that after 10 cycles, the weight loss on the top surface of plain concrete increases dramatically, especially after 40 cycles. The weight loss for the PCC, with $p/c = 22.0\%$ and $w/c = 0.44$, also shows an apparent increase after 10 cycles. A closer observation reveals the peeling of a thin layer of polymer film, formed on the top surface of the concrete after casting (Su 1995). The other concrete specimens show excellent F-T resistance with deicing salt.

Figs. 18 and 19 present the results of the weight loss on the side surface and bottom surface of specimens during the F-T test, respectively. As can be seen from the figures, the surface weight loss of plain concrete and the PCC, with $p/c = 5.7\%$ and $w/c = 0.44$, increases remarkably after the commencement of the F-T test. The surface weight loss is much higher than that of the RILEM requirement (0.2 mg/mm^2), indicating poor F-T resistance with deicing salt. In contrast, the rest of the PCC's, with $p/c \geq 11.2\%$, don't show apparent weight loss. This means that those PCC's are excellent with respect to the F-T resistance with deicing salt.

Figs. 17–19 reveal that the scaling resistance is excellent for the PCC with $p/c \geq 11.2\%$, regardless of the w/c ratio. This is probably due to the formation of a continuous polymer phase throughout the matrix with a polymer content above 10% (Dingley 1974, Evbuomwan 1990 & Lavelle 1988).

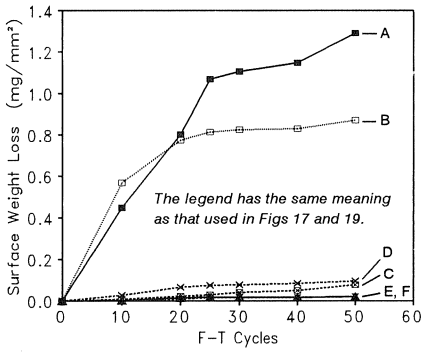

Fig. 18. The side surface weigth loss of concrete specimens as a function of the number of F-T cycles with deicing salt.

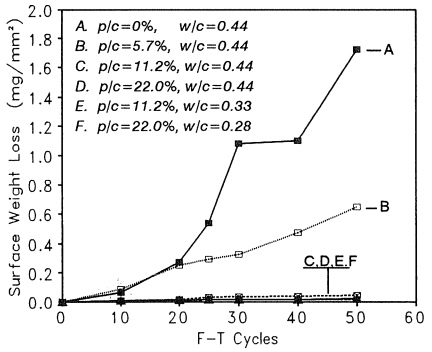

Fig. 19. The bottom surface weigth loss of concrete specimens as a function of the number of F-T cycles with deicing salt.

4.7.3 F-T resistance of PCC's in the absence of deicing salt (mechanical properties)

Fig. 20 shows the results of the transition time of an ultrasonic pulse through specimens as a function of the number of cycles during the F-T test without deicing salt. The change of the transition time can be an indication of the variation of concrete structure caused by the F-T cycling. It can be seen from the figure that the transition time increases with increasing polymer content and decreases with decreasing water/cement ratio. Also, the transition time for various concretes is in the range of 65–75 μs, and nearly remains constant throughout the F-T test (up to 50 cycles).

The results suggest that no apparent damage occurs in the core of all concretes investigated, i.e. all concrete specimens are durable in terms of the F-T test without deicing salt.

Fig. 21 presents the results of the modulus of rupture of concretes. As can be seen from the figure, the modulus increases with increasing polymer contents, with the exception of the PCC with p/c = 22.0% and w/c = 0.44. The fall of the modulus for this specimen appears to be due to segregation. The modulus of rupture generally shows a slight decrease after the F-T test, which is probably due to the increased moisture content. Furthermore, the PCC with p/c = 22.0% and w/c = 0.44 shows the biggest decrease in the modulus as compared with the other specimens.

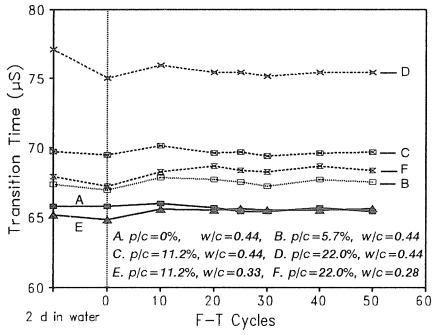

Fig. 20. Effects of the F-T cycles on the transition time of an ultrasonic pulse through concrete specimens.

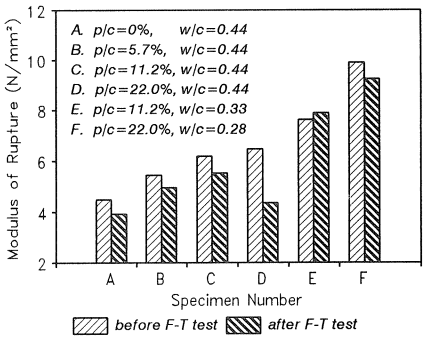

Fig. 21. Effects of the F-T test on the modulus of rupture of concrete specimens.

Fig. 22 shows the effect of the F-T cycling and D-W treatment on the compressive strength of PCC's. The figure demonstrates that the F-T cycling has only a minor effect on the compressive strength, even in the case of No. E and F (with lower w/c), the compressive strength shows a substantial increase after the F-T test. It also can be seen from the figure that for PCC's after the D-W treatment, the compressive strength increases significantly. This appears to be due to the formation of a stronger polymer film. While for the plain concrete, it shows a slight decrease.

In view of the results, all concrete specimens prepared in this investigation are durable with regard to F-T tests with and without deicing salt because there is no apparent increase in the transition time and decrease in the modulus of rupture and compressive strength.

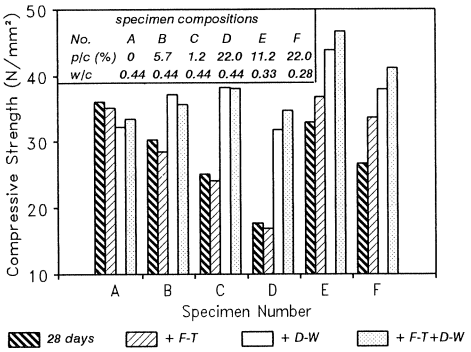

Fig. 22. Effects of the F-T cycles and D-W treatment on the compressive strength of concrete.

5 Discussions

The Coulter and filtration test results show that a part of polymer particles is adsorbed on the surface of cement grains directly after mixing as shown in Figs. 1 and 2. The adsorption has been further confirmed by the ESEM observations as shown in Figs. 5 and 7. This adsorption can be either due to the surface charge of cement minerals (Su et al 1992 & Marshall 1949) or due to the interaction of carbonyl groups ($C = O$) on polymers with Ca^{2+} ions released by the hydration of cement (Su et al 1992 & Larbi et al 1991).

It is apparent that the percentage of polymer particles adsorbed on the surface of cement grains decreases with increasing polymer contents (Su et al 1992). With increasing polymer contents, a larger percentage of polymer particles becomes dispersed in the mixing water. On the assumption that the polymer is adsorbed equally on the cement constituents and there is no considerable amount of hydration products formed after mixing. Then, the average thickness of a polymer layer could be calculated. For the cement with a specific surface of 4000 cm^2/g, and a polymer with an average particle size of 0.27 μm, and a known percentage of the SA polymer adsorbed on cement, the average thickness of the adsorbed polymer layer is shown in Table 3. The thickness of the polymer layer on cement increases with increasing polymer content. The results suggest that the polymer particles (with $p/c \geq 11.2\%$) are able to cover cement completely. This could also explain other results, such as F-T tests with deicing salts.

Table 3. The calculated thickness of polymer layer adsorbed on cement grain based on the results in the literature (Su et al 1992).

polymer contents	p/c	5.7%	11.2%	22.0%
	p/s*	0.14	0.25	0.42
adsorbed polymer (%)		69.3**	62.2	50.4
thickness of polymer film (μm)		0.14	0.26	0.40
numbers of polymer layers		0.53	0.97	1.48

* The volume ratio of polymer solids to the sum of polymer solids and cement

** Based on the filtration test result, the rest based on the Coulter results (Su et al 1992)

The adsorption of polymer particles not only influences the hydration of cement, but also affects the structural evolution of polymer cement pastes. As cement hydration continues, reaction products push the polymer film outward, and eventually penetrate it. This process occurs at about 1 day for the paste with 5.7% of polymer as shown in Fig. 7 (B). However, for the paste with 22.0% of polymer, the surface of cement grains is still almost covered with polymer film at 3 days (Su et al 1995).

The polymer film, formed on the surface of cement grains and hydration products, became thicker at increasing polymer content. Consequently, the polymer film may inhibit the hydration products growing into capillary pores. In the case of increasing polymer content, more and more hydration products are confined in the space between the polymer film and unreacted cement cores, or penetrated into the polymer film and vice versa. This could be the cause for the increase in the volume of big pores (bigger than 1 μm) and the decrease in the volume of small pores (smaller than 0.03 μm) as shown in Fig. 12. The retardation of cement hydration (see Fig. 3) with increasing polymer content could be another reason for the decrease in the volume of small pores.
A previous investigation (Su 1995) has shown that, as cement hydration proceeds, the capillary porosity and total porosity decrease, while the gel porosity increases. It has also revealed that the difference between the theoretically calculated porosity (Su 1995 & Tylor 1990) and the total intruded porosity decreases with increasing polymer content at the same water/cement ratio. This means that the un-intruded pores (with a diameter smaller than 0.0076 μm) decrease with increasing polymer content. This corresponds with the observed coarsening of pore structure due to the polymer addition.

If cement pastes and concretes, with about the same water /cement ratio and polymer/cement content, are compared, e.g. the cement paste, with $p/c = 11.2\%$ and $w/c = 0.30$, and the PCC, with $p/c = 11.2\%$ and $w/c = 0.33$, it is obvious that there is a major difference in the pore size distribution. The volume of pores larger than 1 μm in the concrete is substantially higher, while the volume of pores between 0.1–1 μm is lower. This is likely to reflect the effect of the interfacial zone as shown by Larbi (Larbi 1993).

Based on the Coulter and filtration test results, ESEM and SEM observations and cement hydration data presented at the present paper, a model of the process of the microstructure formation of PCC can be elaborated as follows: Initially, a thin layer of close-packed polymer particles is formed on the surface of cement grains soon after mixing, another part of the polymer particles remains dispersed in the mixing water. Then, as cement hydration proceeds, hydration products are developed in the space between cement grains and the close-packed polymer spheres, which eventually develop into a polymer film. The free polymer particles, dispersed in the free water, are more and more restricted into confined capillary pores and "neck regions" among cement grains. Finally, with water withdrawal by cement hydration and evaporation, the concentrated free polymer particles could fill in areas between cement grains, coalescing into a polymer film. Cement hydration products push the polymer film away and grow through it. Ultimately, a monolithic structure of polymer film interwoven with cement hydration products is developed. A continuous polymer phase throughout the matrix can be formed if the polymer content is equal to or above 10% (Dingley 1974, Evbuomwan 1990 & Lavelle 1988).

1622The present model suggests that adsorbed polymer particles do not play a part in the polymer film formation and will be less effective for the matrix improvement. This could explain the poor results with a polyvinylidene chloride polymer dispersion because of a strong adsorption of polymer on the surface of cement grains as found in previous studies (Su et al 1991b & Su 1995). The efficiency of polymer modification may be improved if less polymer adsorption occurs. In fact, with increasing SA polymer content, the percentage of adsorbed polymer particles decreases, which may increase its efficiency in modifying the matrix, since a larger part of polymer particles in the liquid phase is available for the film formation.

The coarsening effect of the pore structure of PCC does not mean that PCC must have fast water absorption and high water content as it comes into contact with water as compared with the reference concrete. Conversely, the results presented in Figs. 14–16 show that polymer modification significantly reduces the water absorption of concretes. The cause can be due to the hydrophobic characteristic of polymer films formed on the wall of capillary pores (Chandra et al 1987), blocking up the capillary pores. The reduction of water absorption undoubtedly is beneficial for the F-T resistance of concretes. The effect of this phenomenon is that when concrete freezes, the water content of PCC will be lower than that of the unmodified. Consequently, the resistance to freezing-thawing will be higher (Fagerlund 1974). A previous study has also shown that the F-T cycling has only a minor effect on the pore structure of PCC (Su 1995).

In view of the proposed model, the improvement in the mechanical properties, scaling resistance due to polymer addition can be attributed to the following causes:

* An important contribution is probably due to the decrease of the water absorption at increasing polymer content owing to forming a continuous polymer film throughout the matrix. This means that at freezing the probability that the water saturation degree is higher than the critical value may be diminished;
* A relatively amount of polymer present at the interface improves the adhesion strength of cement matrix to aggregates;
* The polymer film formed in PCC's acts as an expansion vessel because the soft polymer is easily pushed away by expanding water and ice, depending on the minimum film formation temperature and glass-rubber transition temperature of the polymer;
* The strain capacity, toughness and tensile strength are increased at increasing polymer contents.

All concretes investigated appear to be resistant to the F-T regime (without deicing salt). Apparently the F-T test regime applied is insufficiently discriminative. On the other hand, frost-thaw damage does not occur in the Netherlands for the concretes with the w/c ratios tested.

6 Conclusions

The results have revealed that a part of polymer particles is adsorbed on the surface of cement grains directly after mixing, the percentage of the adsorbed polymer decreases with increasing

polymer contents. The adsorbed polymer particles can form a polymer film on the surface of cement grains. The thickness of the polymer film increases with increasing polymer content. Non-adsorbed polymer particles, dispersed in the liquid phase, can form a polymer film between cement grains.

It is found that with increasing polymer content at a constant water cement ratio, the total intruded pore volume of cement pastes decreases, whereas for concrete it shows a substantial increase. In this case, the pores become more coarse. A decrease in the total intruded volume and the volume of the pores larger than 1 μm is observed for PCC's with the same workability as that of the reference concrete. This is due to the substantial reduction of water cement ratio.

The adsorption of polymer particles not only retards the hydration of cement, but also influences the structural evolution of polymer cement pastes. Based on the results of the Coulter analysis, cement hydration data, the ESEM and SEM observations of cement pastes, a model of the evolution of the microstructure is proposed. Based on this model, the polymer film can be formed in the capillary pores and at the aggregate-paste interface, the weakest points in the concrete, where the polymer film plays an important role with respect to the adhesion, and consequently has a positive effect on strength. Thus, the mechanical properties improve.

PCC's with a polymer content of 11.2% or more are F-T deicing salt resistant according to the RILEM Recommendation: "Methods of carrying out and reporting freeze thaw tests with deicing chemicals". But for the PCC with $p/c \leq 5.7\%$, the scaling resistance does not meet the RILEM requirement because a continuous polymer film is hardly formed in the matrix. The improvement in the mechanical properties and the F-T resistance of PCC cannot be explained by the change in the pore structure of PCC's, however, it must be associated with a substantial decrease in the water adsorption during the F-T testing.

References

BENTUR, A. (1990), The Effect of in situ Polymerization on the Chloride Diffusion and Microstructure of Polymer Portland Cement Pastes and Mortars, *Advance in Cement Research*, No. 9, pp. 1–7.

BIJEN, J.M.J.M. (1991), Polymeren in Beton, *Cement*, No. 5, pp. 60–69.

BIJEN, J.M.J.M. (1994) Personal communication.

CHANDRA, S. and FLODIN, P. (1987), Interaction of Polymer and Organic Admixtures on Portland Cement Hydration, *Cement and Concrete Research*, Vol. 17, pp. 875–890.

DINGLEY, R.G. (1974), *The structure and properties of hydraulic cement paste modified by polymer latex*, Dissertation, University of Southampton.

EVBUOMWAN,N.F.O. (1990), A State of the Art Report on the Strength and Durability properties Polymer Modified Mortars and Concrete, *The Proceedings of 6th ICPIC*, China, pp. 52–59.

FAGERLUND, G. (1977), The Critical Degree of Saturation Method of Assessing the Freeze/Thaw Resistance of Concrete, *Materiaux et Constrctions*, Vol. 10, pp. 217–229.

FRAAIJ, A.L.A. (1990), *Fly Ash a Pozzolan in Concrete*, Ph.D Thesis, TU Delft.

FRANKE, V.B. (1941), Bestimmung von Calciumoxyd und Calciumhydroxyd neben Wasserfreiem und Wasserhaltigem Calciumsilikat, *Zeitschrift fur anorganische und allgemeine Chemie*, Band 247, pp. 180–184.

GROOKURTH, K.P. (1989), Morphology and Long Term Behaviour of Polymer Cement Concrete, *MRS Symposium Proceedings*, Vol. 179, pp 273–281.

ISENGERG, J.E. and VANDERHOFF, J.W. (1973), A hypothesis for the reinforcement of Portland Cement by Latex, *Am. Chem. Soc. Polymer Reprints*, Vol. 14, No. 2, pp. 1197.

LAVELLE, J.A. (1988), Acrylic Latex-Modified Portland Cement, *ACI Materials Journal*, pp. 41–47.

LARBI, J.A. (1993), Microstructure of Interfacial Zone around Aggregate Particles in Concrete, *HERON* Vol. 38, No. 1.

LARBI, J.A. and BIJEN, J.M.J.M. (1991), Interaction of Polymers with Portland Cement during Hydration: The Chemistry of the Pore Solution of Polymer-Modified Cement Systems, *Cement and Concrete Research*, Vol. 20, pp. 139–147.

LAVITT, M. (1974), Methods of carrying and reporting Freeze / Thaw Tests on Concretes, *Materiaux et Constructions*, Vol. 7, pp. 355–359.

LEFEBURE, V. (1924), "British Patent" No. 217, 279.

MAI, Y.W. and COTTERELL, B. (1986), Porosity and Mechanical Properties of Epoxy Resin Modified Cement Mortar, *Cement and Concrete Research*, Vol. 16, No. 5, pp. 646–652.

MARSHALL, C.M. (1949), *The colloid chemistry of the silicate minerals*, Academic Press Inc. Publishers. Nany, E.G., Ukadike, M.M. and Souer, J.A. (1978), Optimum Polymer Contents in the concrete modified by liquid epoxy Resins, *Polymer in Concrete ACI SP-58*, Detriot, USA, pp. 329–355.

OHAMA, Y. (1987), Principle of Latex Modification and Some Typical Properties of Latex-Modified Mortars and Concretes, *ACI Materials Journal*, pp. 511–518.

POPOVICS, S. and TAMAS, T. (1978), Investigation on Portland Cement Paste and Mortars Modified by the Addition of Epoxy, *Polymer in Concrete ACI SP-58*, Detroit, USA, pp. 357–367.

SU, Z. (1994) The Microstructure and Properties of Polymer Modified Cement Concrete, *Deutscher Ausschuss für Stahlbeton - 29. Forschungskolloquium Proceedings*, pp.195–202.

SU, Z. (1995), *Microstructure of Polymer Cement Concrete*, Ph.D thesis, TU Delft, Published by Delft University Press, ISBN: 90-407-1083-X.

SU, Z. and BIJEN, J.M.J.M. (1990), The Effect of Polymer Dispersions Modification on the Interface between Cement Paste and Aggregates, *The Proceedings of 6th ICPIC*, pp. 474–481.

SU, Z., BIJEN, J.M.J.M. and FRAAIJ, A.L.A. (1992), The Interaction of Polymer Dispersions with Portland Cement Paste, *MRS Symposium Proceedings*, Vol. 289, pp. 199–204.

SU, Z., BIJEN, J.M.J.M. and FRAAIJ, A.L.A. (1992a), A SEM Study of Polymer Modified Cement Paste and Its Interface with Limestone, TU delft, *Stevin Report 25.1-92-11*.

Su, Z., BIJEN, J.M.J.M. and FRAAIJ, A.L.A. (1993), The Evolution of the Microstructure in the polymer Modified Cement Paste at the Early Stage of Cement Hydration, TU Delft, *Stevin Report, 25.1-93-03*.

SU, Z., BIJEN, J.M.J.M. and FRAAIJ, A.L.A. (1994), The Effect of Freeze-Thaw Cycles on the Pore Structure of Polymer Cement Paste and Concrete, TU Delft, *Stevin Report 25.1-94-05*.

SU, Z., BIJEN, J.M.J.M. and LARBI, J.A. (1991a), The Influence of Polymer Modification on the Hydration of Cement, *Cement and Concrete Research*, Vol. 21, pp. 535–544.

Su, Z., Bijen, J.M.J.M. and Larbi, J.A. (1991b), The Influence of Polymer Modification on the Adhesion of Cement Paste to Aggregates, *Cement and Concrete Research*, Vol. 21, pp. 726–736.

Su, Z., Larbi, J.A. and Bijen, J.M.J.M. (1991), The Interface between Polymer Modified Cement Paste and Aggregates, *Cement and Concrete Research*, Vol. 21, pp. 983–990.

Su, Z., Sujata, K., Bijen, J.M.J.M., Jennings, H.M. and Fraaij, A.L.A. (1995), The Evolution of the Microstructure in Styrene Acrylate Polymer-Modified Cement Pastes at the Early State of Cement Hydration, *Advanced Cement Based Materials*, Vol.2, No.6, pp.--.

Taylor, F.H.W. (1990), *Cement Chemistry*, Academic Press Limited, NSBN 0-12-683900-X.